공학석사학위논문

Transparent Kirigami Electrodes for Electronic Skin Applications

전자피부 어플리케이션을 위한 투명 키리가미 전극 개발

2019년 2월

서울대학교 대학원

기계항공공학부

박 정 재

Transparent Kirigami Electrodes for Electronic Skin Applications

지도교수 고 승 환

이 논문을 공학석사 학위논문으로 제출함
2018년 10월

서울대학교 대학원
기계항공공학부
박 정 재

박정재의 공학석사 학위논문을 인준함
2018년 12월

위 원 장 김 찬 중 (인)

부위원장 고 승 환 (인)

위 원 송 한 호 (인)

Abstract

For relieving the inconvenience while wearing electronic devices, stretchability and imperceptibility are essentially required characteristics for desired form of electronic-skin devices. Yet accomplishing these properties simultaneously is still challenging although some progress has been made on materials and structure designs. Here, we suggest a novel fabrication technique brining an idea from kirigami, Japanese ancient paper-cutting craft, to enable transparent and highly conductive electrodes to be deformable. By using facile and fast laser patterning process, we show transparent kirigami electrodes composed of silver nanowires partially embedded in ultra-thin colorless-polyimide film. Owing to rapid laser patterning method, versatile patterns are developed in few minutes under non-vacuum and room temperature condition. These patterns impart tunable elasticity to the electrodes, which can be stretched over 400% tensile strain with strain-invariant electrical property and also show good electromechanical stability even after 10,000 cycles of 400% stretching while exhibiting high optical transparency (more than 80%). In addition, gold coating on the exposed surface of silver nanowires ensure biocompatibility and improved electrical stability, preventing allergic reaction of skin and oxidation of the silver nanowires. The transparent kirigami electrodes with customizable elasticity pave the innovative way that offers facile construction of appropriate geometries for achieving multi-functional transparent and wearable electronic skin applications. The versatility of this work is demonstrated by ultra-stretchable transparent kirigami heater for personal thermal management and conformal transparent kirigami electrophysiology sensor for continuous health monitoring of human body conditions. Finally, by integrating electronic-skin sensors

with a quadrotor, we have successfully demonstrated human-machine interface using our stretchable transparent kirigami electrodes.

Keyword : Transparent, Conformal, Stretchable electronics, Silver nanowire, Electronic skin

Student Number : 2017-20632

Table of Contents

List of Figures

Figure 6. Mechanical characterization of transparent kirigami electrodes with various uniaxial kirigami pattern. a-c) Experimental stress-strain curves of varying kirigami geometries and **d-f)** corresponding electromechanical performance with the elongations. Unit cell of uniaxial pattern and three key parameters of the unit cell in the insets in **a-c)**. Actual cutting lines are marked as black lines.

Figure 7. Electromechanical stability of transparent kirigami electrode with uniaxial kirigami pattern. Resistance change versus the number of cyclic stretching of TKE under the tensile strain of 400%. Magnified regional resistance change under cyclic stretching shown in the dashed red box.

Figure 8. Demonstration of transparent kirigami heater. a) Schematic illustration of uniaxial TKH (cutting dimensions: L_c = 15 mm, x = 1.7 mm, and y = 1.7 mm). **b)** Wearable TKH that operates on the wrist at input voltage of 4.5 V and performs under dynamic movements (upward and downward).

Figure 9. Electrothermal performance of transparent kirigami heater. a) Maximum temperature at increasing input voltages from 1.5 V to 9.0 V. **b)** Cyclic operation temperature at 6 V. **c)** Resistance versus temperature of calculated and measured graph of TKH.

Figure 10. Transparent kirigami EP sensor. Schematic illustration of TKE for capturing various EP signals. TKEs are patterned as Ref., GND., and Mea. electrodes with biaxial pattern with the additional thin Au-coated layer**.**

Figure 11. Various EP signal measurements using transparent kirigami EP sensor. Different EP signals from various locations for **a)** EEG, **b)** EOG, **c)** EMG, and **d)** ECG. Schematic illustration of measurement locations on graphical human model for monitoring EEG signal and EEG alpha-rhythms observed around 10 Hz in **a)**. Real images of measurement locations for other EP signals in **b-d)**.

Figure 12. Human-machine interface using transparent kirigami electrodes. Schematic illustration of demonstrating HMI through TKEs by controlling a quadrotor with the gestures, which are signal-processed by Bluetooth and WiFi network.

Figure 13. Demonstration of human-machine interface via transparent kirigami electrodes. a) Two measured EMG signals from both forearms using transparent kirigami EP sensors. Roman numbers enclosed in the orange box under the signals represent corresponding commands in **b)**. **b)** Description of control motions and corresponding gestures: i) Take off, ii) Fly forward, iii) Turn left, iv) Turn right, v) Land.

Chapter 1. Introduction

1.1 Study Background

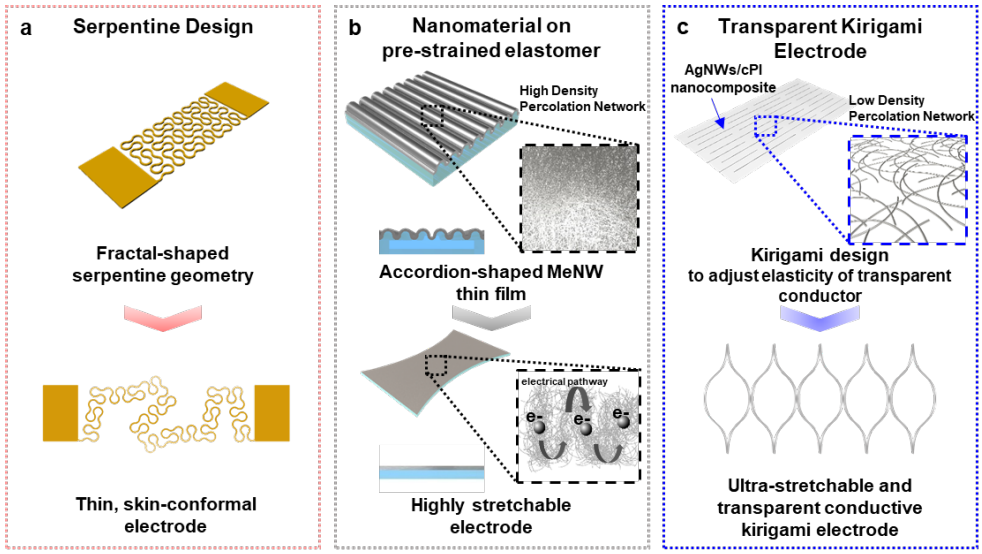

Figure 1. Comparison of methods for fabricating stretchable electrodes. a) Serpentine design. **b)** Nanomaterial on pre-strained elastomeric substrate. **c)** Our kirigami approach to generate electrode that is both stretchable and transparent.

Electronic-skin (E-Skin) that can detect and monitor biopotentials while having conformal integration onto the skin is a desired form of delivering mechanical/electrical stimulus into quantitative electrical signals[1], and its investigations are extensively on-going for human-machine interface (HMI)[2], soft robotics[3, 4], and continuous personal healthcare monitoring system in the field of ICT/IoT[2, 5-7]. Two essential characteristics, conformability and imperceptibility, are crucial when developing E-Skin to provide precise measurement of bio-signals directly from the surface of skin[8] and to look imperceptible to human-naked eyes

in forms of a tattoo[9], a bandage[10], and a skin-replacement[11-15]. However, achieving stretchability and transparency simultaneously in high tensile strain (>50%) without degradation of electrical and mechanical properties is currently very challenging even with extraordinary properties of nanocomposites[16], stretchable serpentine structure[17], pre-strained[18] and ultra-thin substrates[11, 19-21], as depicted in **Figure 1**. Although investigations of structural design to grant stretchability in flexible electronics have been widely demonstrated by serpentine or horseshoe structure[22], making appropriate structure to avoid generation of large or irreversible cracks in certain strain region (usually falls within 20~50%) is only achieved[9, 23-25]. Nevertheless, transparency and electrical conductivity is limited. Thus, with increasing demands of multi-functional, wearable devices[6, 8, 17], E-skin devices must comprise characteristics that are mechanically stable under large tensile strain (>50%) and transparent at the same time[26-28].

1.2 Purpose of Research

To achieve transparent and stretchable electrodes, we show a simple strategy that is learned from the ancient art of repetitive paper cutting called kirigami[29-32]. In this research, the electrodes are fabricated rapidly with an aid of laser ablation technique, an advanced manufacturing process that uses pulsed UV irradiations in nanosecond intervals[33]. By varying the cutting parameter on computer-aided design (CAD) program[33], we are able to modulate the strain elongation of conductive nanocomposite materials that is even transparent without generation of patterning masks and fabrication steps in conventional photolithography process[33]. The electrodes used in this research generally consist of silver nanowires (AgNWs) and ultra-thin colorless-polyimide (cPI) layer (<5 μm) to ensure high optical, thermal, electrical properties and biocompatibility. Transparent kirigami electrode (TKE) fabricated using our method enables tunable elasticity by constructing micro/nano-mesh[4, 29], which can elongate from even small strain of 0% and up to ultra-high strain of 400% with negligible mechanical hysteresis (under 3%) and good strain reversibility even after 10,000 cycles of stretching while exhibiting optical transparency of >80%. Demonstration of stretchable and transparent kirigami heater that elongates up to high strain of 200% shows the capabilities of personal thermal treatment[16, 23, 24], wearable thermal haptic[34], and wound healing monitoring[17] that usually require large-dynamic mechanical deformations[35]. Characteristic of soft and thin but ultra-stretchable properties of TKE enables to capture various electrophysiology (EP) signals on curvilinear and irregular surfaces of human body (for example, forehead, temple, forearm, etc.)[9, 19, 20, 36, 37]. Long-term monitoring of EP signals using the electrode is realized by coating non-toxic, oxidization resistant

material, in this case gold (Au), on the exposed surface of AgNWs[4]. Enhanced electrical stability under environmental/sweating condition after galvanic coating process of Au[38] also assists stable long-term monitoring of the electronics[6]. Finally, the versatility of our E-skin sensor is demonstrated by skin surface electromyogram (sEMG) on both forearms that are measured in real time to use the body motions for controlling a quadrotor in an advanced form for the demonstration of HMI[2, 39].

Chapter 2. Experiment

2.1 Fabrication of Transparent Kirigami Electrodes

General fabrication process of TKE is illustrated in **Figure 2a**. On a glass substrate, AgNWs are deposited using vacuum filtration process, and cPI varnish (Kolon Industries, Korea) in DMSO is spin-coated over the area. By utilizing UV pulsed laser ablation process, both AgNWs and cPI layers are patterned rapidly at the same time in desired-shaped kirigami structure. **Figure 2b** shows SEM images of various 2D micro-patterns on AgNWs/cPI layer in shapes of uniaxial, biaxial, and square spiral respectively. Each shape exhibits stretchable configuration that have unique characteristics for different applications. Finally, the patterned AgNWs/cPI nanocomposite with kirigami structure is easily peeled from the substrate. Detailed material choices, important experimental parameters and fabrication processes are described in latter discussion.

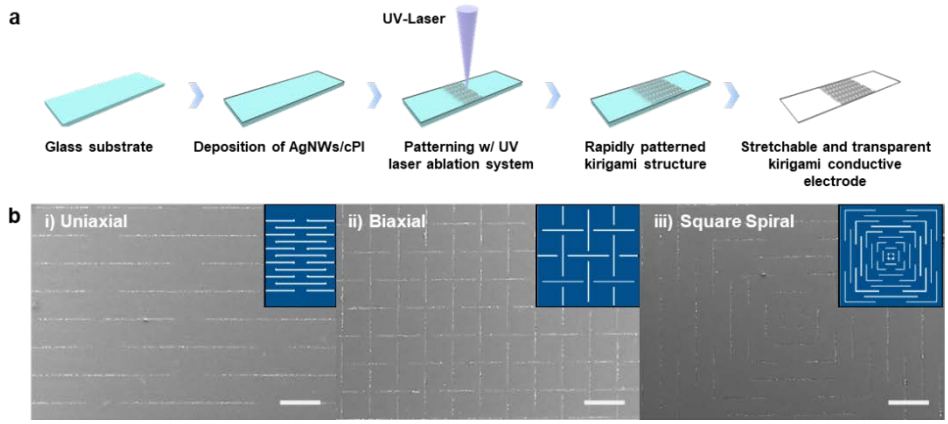

Figure 2. Fabrication of transparent kirigami electrode based on AgNWs transparent conductor embedded in cPI film with various patterns. a) Brief fabrication process of transparent kirigami electrodes that is employed throughout the experiments. **b)** SEM images of various kirigami structures and their 2D designs in the inset: i) Uniaxial, ii) Biaxial, iii) Square spiral (Scale bars are 200 μm).

2.2 Synthesis of Silver Nanowires

Synthesis of relatively long AgNWs (~100 μm in length, ~100 nm in diameter) employs a modified polyol method using a one-pot process. In the process, all reagent chemicals are put into a triangular flask at once, which offers a simple and facile synthesis of long AgNWs[40]. In 50 mL of ethylene glycol (EG), 0.4 g of polyvinylpyrrolidone (PVP, Mw ~ 360,000, Sigma Aldrich) and 0.5 g of silver nitrate ($AgNO_3$) are sequentially dissolved using a magnetic stirrer. The stirrer is carefully removed from the mixture solution after all reagents are completely dissolved. As a following step, 800 μL of copper(II) chloride dihydrate solution ($CuCl_2 \cdot 2H_2O$, Sigma Aldrich, 3.3 mM dilution with EG) is rapidly injected into the mixture solution and gently stirred by a hand. Finally, the reaction flask containing the mixture solution is placed into a preheated silicone oil bath at 130°C, where AgNWs in the mixture grow at the elevated temperature for 3 h. Once sufficient growth of AgNWs have been achieved, the final solution is cleaned using acetone and ethanol to remove the chemical residues along with centrifugation of 3000 rpm for 10 min, and this process is repeated three to four times. The purified AgNWs are re-dispersed in ethanol for the use.

2.3 Fabrication of AgNWs/cPI Electrodes

Depending on the desired transparency and electrical conductance of AgNWs transparent conductor, proper amounts of AgNWs dispersed in ethanol are transferred on a glass substrate by vacuum filtration method. Usually, 300 μL of AgNWs dispersed in ethanol (~0.015 wt%) is used for the deposition of AgNWs throughout experiments. The transferred AgNWs are thermally annealed on a hotplate at 200 °C for 30 min. Onto the annealed AgNWs, cPI varnish is spin-coated at 700 rpm for 60 seconds and baked sequentially at 150°C for 5 min and 260 °C for 30 min. The fully cured AgNWs/cPI nanocomposite is patterned by utilizing UV-laser ablation method. The kirigami patterned AgNWs/cPI composite electrode is carefully peeled off from the glass with a water-soluble tape (Aquasol Corp., North Tonawanda, NY) attached on the top and dissolved. Thus, the resultant electrode is composed of the AgNWs that are embedded in the cPI thin film with partially exposed part of the AgNWs.

2.4 Laser Ablation Patterning Process

The AgNWs/cPI electrode on the glass substrate is irradiated with a Q-switched DPSS laser to ablate the electrode along kirigami pattern. The laser operates at the wavelength of 355 nm, the pulse repetition rate of 30 kHz and the pulse width with 35 nanoseconds. By using a 2-axis Galvano mirror scanner, the beam spot successfully follows a desired kirigami pattern delivered from CAD program. The focused beam spot width is approximately 20 μm so the ablated spot diameter falls under 20 μm. The control parameters repetitions, current power %, and scanning speed are carefully adjusted to ablate the desired patterns.

2.5 Gold Coating on The Exposed AgNWs

Gold layer is coated on the exposed AgNWs of TKE by the galvanic replacement process modified from previous study[38, 41]. The first step of Au coating by the galvanic replacement process involves placing patterned TKE in gold(III) chloride trihydrate solution ($HAuCl_4 \cdot 3H_2O$, Sigma Aldrich, 0.3 mM dilution with deionized water) for 10 min. Followed by the replacement process, the TKE is dipped in 28 % of aqueous solution of ammonia (NH_4OH, Sigma Aldrich) for 1 min to remove silver chloride (AgCl) produced around the Au-AgNWs. **Figure 3a** shows that exposed surfaces of AgNWs are selectively coated with Au via comparison between two EDS images of ii) Ag only and iii) Au only. The Au layer contributes as oxidization-resistive and conductive layer (**Figure 3b-c**).

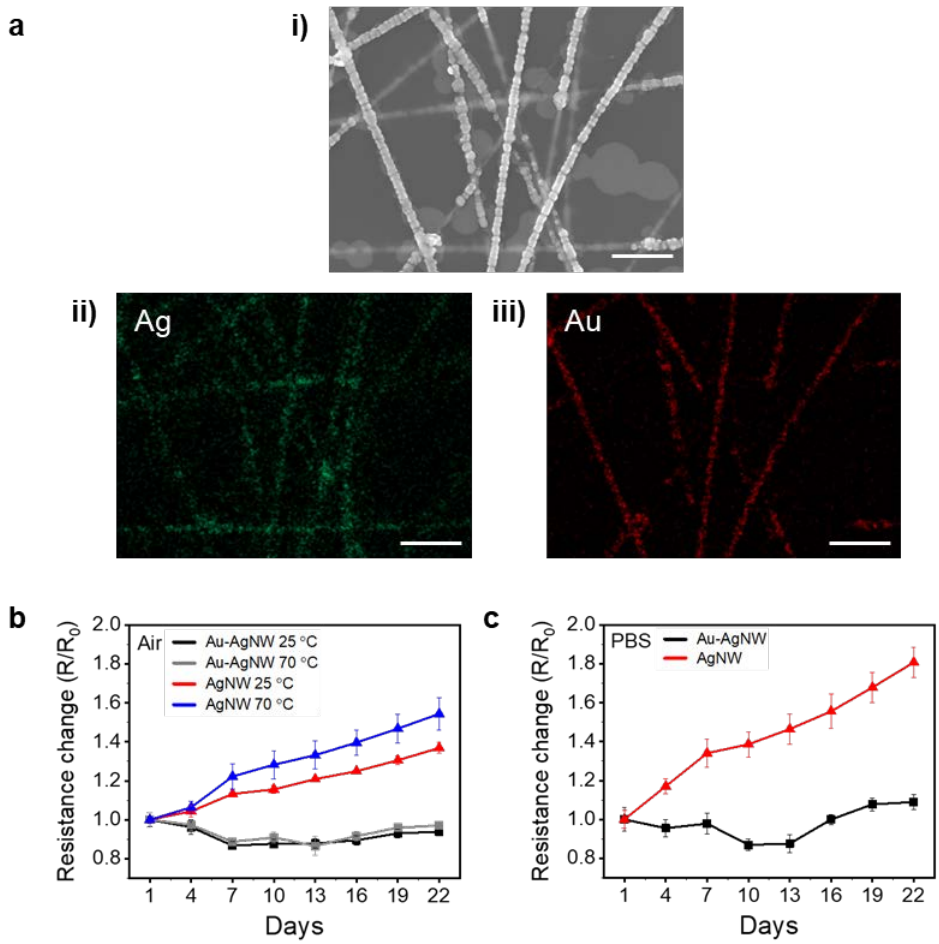

Figure 3. Selective Au-coating on the exposed surface of AgNWs. a) EDS images that show Au layers coated selectively on the exposed surface of AgNWs: i) SEM image, ii) Ag only, iii) Au only (Scale bars are 1 μm). Oxidization stability test **b)** in thermally accelerated condition and **c)** in PBS solution.

2.6 Finite Element Simulation

Finite element method (FEM) provides the mechanical deformation behavior and the stress distribution of the stretched structures with various kirigami pattern designs. Free triangular element is chosen as a mesh of which size ranges from 0.01 mm to 0.15 mm. We use two techniques to avoid bifurcation of the buckling: (1) one is related to a boundary condition and (2) another one is in a study method. We set a prescribed displacement boundary condition at both ends of the structures. The boundary condition consists of not only displacement in the axial direction but also displacement perturbation in the plane-normal direction. Because the size of the perturbation is close to 0.1 % of the minimum element size, it does not have significant effect on the stress-strain relationship. Furthermore, we apply an auxiliary sweep method so that the simulating calculation runs with the incrementally increasing displacement value. These techniques help the buckling occurs in the one direction.

Chapter 3. Result

3.1 Characterization of Transparent Kirigami Electrodes

Although diverse kirigami patterns can be constructed by our laser patterning process, uniaxial pattern is employed to study basic understanding of kirigami structures. For investigating mechanical characteristics of TKE with uniaxial kirigami pattern, we analyze mechanical behavior by observing stress distribution of the TKE under strain by running FEM. **Figure 4** presents out-of-plane buckling deformation of the uniaxial TKE under tensile strain from 0% to 200 % in real and FEM snapshots. The matched results of experimental and simulation images indicate that the TKE can be elongated to 200 % without a fracture, and the applied stress is well distributed throughout the TKE.

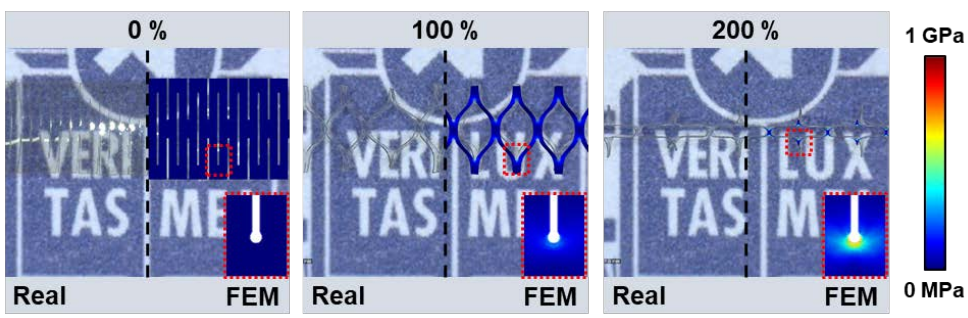

Figure 4. Mechanical behavior of uniaxial transparent kirigami electrodes. FEM images showing stress distribution of TKE with uniaxial pattern under various tensile strains and corresponding real images. Magnified FEM images of stress-concentrated region under each strain in the insets.

Furthermore, cutting edges of the pattern is blunt because the Gaussian energy dispersion of laser beam ablates the electrode along the shape of circular beam spot [33, 42], the laser process assists the distribution of stress effectively without additional setting. This circular edge impedes the growth of crack, therefore allowing to withstand higher strain with the circular edge than the squared edge as shown in their stress-strain curves (**Figure 5**)[29].

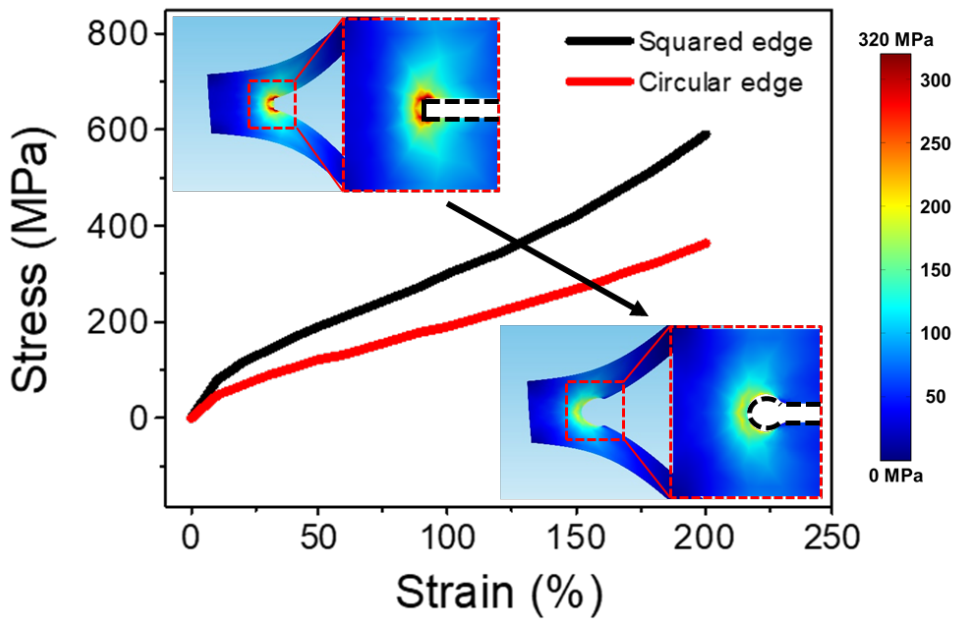

Figure 5. Cutting-edge analysis with COMSOL simulation. The inherited circular edge generated by UV-laser patterning process induced less stress concentration compared to the squared edge.

The unit cell of the uniaxial pattern contains three key parameters: L_c is the cut length, x is the spacing in the horizontal direction and y is the distance in the vertical direction (**Figure 6a-c**, insets). In this case, the theoretical maximum strain before failure can be attained as equation (1), where ΔL is the incremental length and L_0 is

the original length before stretching[43].

$$\%\ \text{strain} = \frac{\Delta L}{L_0} \times 100\ \% = \frac{(L_c - x)}{2y} \times 100\ \% \quad (1)$$

The equation suggests that the unit cell parameters control mechanical properties of structures although it does not consider buckling and torsion that actually occur. To examine the effects of each parameter on the mechanical behavior experimentally, we perform tensile test on the TEKs with various parameters. With handy configurability of the laser patterning process, we could be able to thoroughly study geometrical dependency by easily varying the cutting parameters. In general, the maximum strain increases as L_c increases while x and y decrease, as estimated from the equation (1) (**Figure 6a-c**). The flat and horizontal stable-resistance region, where the resistance does not change, becomes longer as L_c increases and both x and y decrease (**Figure 6d-f**). Because the change in kirigami structure does not induce mechanical deformation of the embedded AgNWs percolation network in the region, there is not the change in electrical resistance while still on-going out of plane deflection. However, at higher strain above theoretical maximum strain, the cut edges start to tear apart from the due to concentrated stress, resulting in damage to the main body of AgNWs/cPI layer that leads to the increase in the resistance[29, 35, 44, 45].

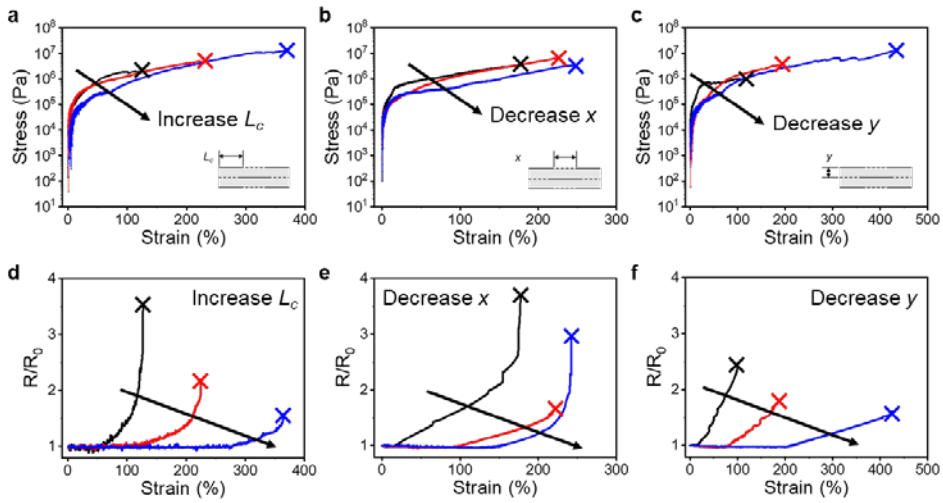

Figure 6. Mechanical characterization of transparent kirigami electrodes with various uniaxial kirigami pattern. a-c) Experimental stress-strain curves of varying kirigami geometries and **d-f)** corresponding electromechanical performance with the elongations. Unit cell of uniaxial pattern and three key parameters of the unit cell in the insets in **a-c)**. Actual cutting lines are marked as black lines.

The other key feature of the TKE is reversibility. As mentioned from the above, TKE have strain-invariant electrical resistance region during one-time stretching; moreover, the resistance lasts constantly under the broad range of strain (0% to 400%) and repeats for 10,000 cycles (**Figure 7**). The shape of TKE returns to the original structure and the resistance change is negligible within 3% on initial resistance even after 10,000 stretching cycles. These electrically invariant and stable while mechanically reversible features of TKE show possibilities of a vast range of electronic skin applications as it can change shapes, modulus and configurability without degradation of electrical performance.

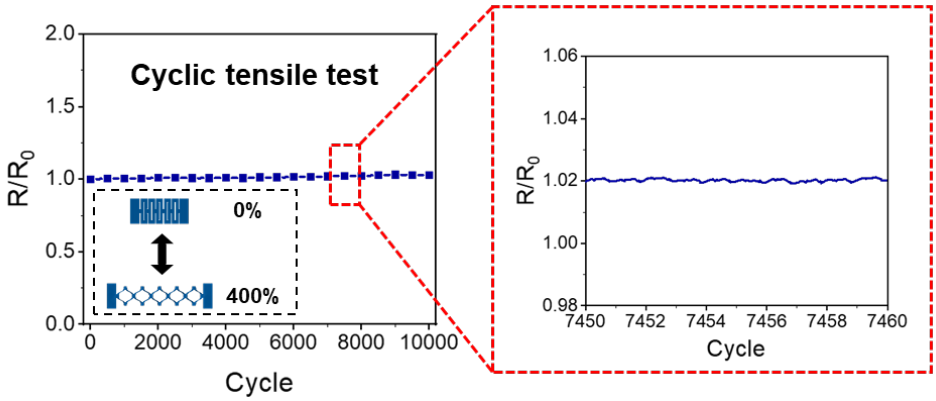

Figure 7. Electromechanical stability of transparent kirigami electrode with uniaxial kirigami pattern. Resistance change versus the number of cyclic stretching of TKE under the tensile strain of 400%. Magnified regional resistance change under cyclic stretching shown in the dashed red box.

3.2 Highly Stretchable and Transparent Kirigami Heater

As a demonstration of E-skin application, we design and fabricate a transparent kirigami heater (TKH) to suggest the feasibility of personal thermal treatment[16, 23, 24], wearable thermal haptic[34], and wound healing monitoring[17]. **Figure 8a** illustrates a schematic structure of the TKH with an enough large area that can cover a wrist of an adult subject. The TKH consists of two layers: (1) a heating layer composed of AgNWs/cPI composite and (2) an encapsulation layer as cPI layer only. The thin encapsulated layer prevents current leakage but facilitates the heat flow. The whole layers are patterned along parallel cut and shaped into uniaxial kirigami structure. The fabricated TKH operates well over a broad range of strains and deformations occurring from dynamic movements such as stretching, bending and twisting. Besides, the TKH shows great structural reversibility and stable electrothermal performances maintaining optical transparency (**Figure 8b**). Because the TKH is designed to stretch out over hundred percentages of strain elongation, it is able to provide thermal treatment over the large area of the skin.

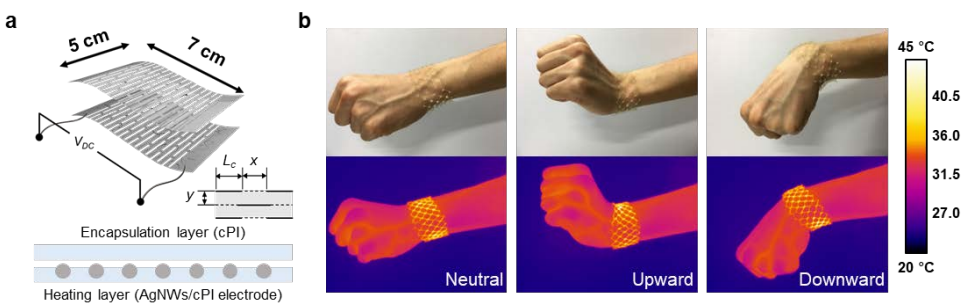

Figure 8. Demonstration of transparent kirigami heater. a) Schematic illustration of uniaxial TKH (cutting dimensions: L_c = 15 mm, x = 1.7 mm, and y = 1.7 mm). **b)** Wearable TKH that operates on the wrist at input voltage of 4.5 V and performs under dynamic movements (upward and downward).

The maximum temperature profiles presented in **Figure 9a-b** show time-domain temperatures by incremental input voltages from 1.5 V to 9.0 V (**Figure 9a**) and repetitive voltage of 6.0 V (**Figure 9b**). At an elevated temperature of ~80 °C, the TKH operates stably without degradation of the electrothermal performance and it gives fast enough thermal response during repetitive voltage on-off cycles. Commonly used conductive materials, especially copper and silver, tend to increase in the resistance respect to the increase in temperature. The TKH is also capable of responding to the change in the electrical resistance of a material depending on temperature since the TKH consists of AgNWs. The TKH shows the positive linear relationship between the resistance and the temperature. Therefore, the constant *dV*/*dT* extracted from the slope of input voltage versus the output temperature graph is used to find out the calculated temperature from the measured resistance as presented in **Figure 9c**. Thus, it suggests a distinctive performance of TKE as a wearable temperature sensor measuring human body temperature in real time[46].

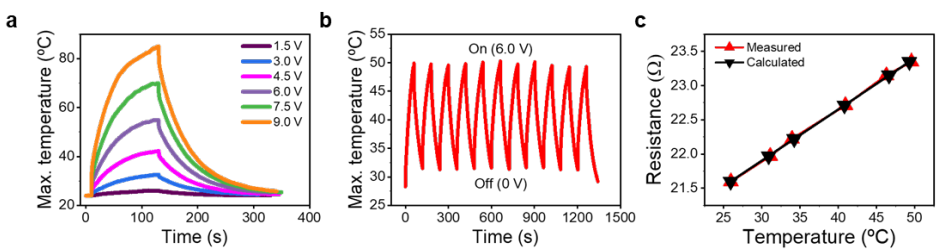

Figure 9. Electrothermal performance of transparent kirigami heater. a) Maximum temperature at increasing input voltages from 1.5 V to 9.0 V. **b)** Cyclic operation temperature at 6 V. **c)** Resistance versus temperature of calculated and measured graph of TKH.

3.3 Conformal and Transparent Kirigami Electrophysiology Sensor

Healthcare monitoring of human body conditions in comfortable and imperceptible way is critically important parts that E-skin devices should take care[4, 9, 12, 15, 19, 21]. **Figure 10** illustrates the conformal and transparent kirigami EP sensor with a set of three discrete electrodes in the shape of rectangular bars, as reference, ground and measure to acquire high-quality EP signals from nearly any region of the body. Basically, the TKE composed of AgNWs/cPI are patterned in biaxial kirigami and then only AgNWs surface exposed out of cPI layer is selectively replaced with a thin Au layer (detailed method described in **Experiment** section) to ensure transparency, conformity and biocompatibility for long-term health monitoring. Because the Au layer protects the AgNWs from oxidization and also improves biocompatibility by preventing allergic reaction of skin[47], the long-term monitoring of EP signals is enabled by utilizing the transparent kirigami EP sensor (**Figure 3b**).

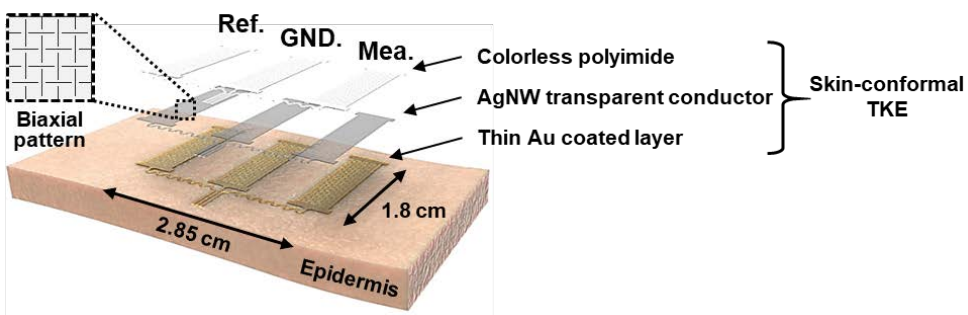

Figure 10. Transparent kirigami EP sensor. Schematic illustration of TKE for capturing various EP signals. TKEs are patterned as Ref., GND., and Mea. electrodes with biaxial pattern with the additional thin Au-coated layer**.**

Figure 11a-d show four sets of images of measuring locations and measured EP signals such as electroencephalography (EEG), electrooculogram (EOG), electromyogram (EMG), and electrocardiogram (ECG) at head, temple, flexor carpi, and heart respectively. For monitoring EEG signal, a separated set of three TKEs are prepared and placed on forehead, shoulder and the area in between auricle and mastoid the works as reference, ground, and measurement electrodes respectively (as illustrated in 3D human model in **Figure 11a**)[6]. **Figure 11a** also offers EEG spectrogram of alpha-rhythm at 8~12 Hz frequency clearly appearing in the relaxed state of human body (classified by opening/closing of eyes)[6, 9]. The spectrogram of EEG is derived by employing short-time Fourier transform (STFT) with software in MATLAB (R2018b, Mathworks, Natick, MA). The EOG signal from blinking of an eye is collected using a miniature set of TKEs on the temple near an eye (real image at left in **Figure 11b**)[48]. The number of blinking is easily classified by observing the number of potential peaks from EOG signals (signal at right in **Figure 11b**). In order to measure surface EMG (sEMG) signal, the transparent kirigami EP sensor is put on a forearm (**Figure 11c**, right). Contraction of flexor carpi in flexion clearly offers large potential difference whereas its extension shows relatively small potential in sEMG signal (**Figure 11c**, left). For measuring ECG signals, the kirigami EP sensor is placed on a chest near the heart to read the rate and rhythm of heartbeats in typical form of QRS signal (**Figure 11d**)[49].

All measurements of the EP signals are collected by using the BioRadio wireless physiology monitor (Great Lakes NeuroTechnologies, Independence, OH). The sampling rate is 1 kHz and gain is 1,000 for amplifying the EP signals. During forearm extension and flexion, the magnitude of sEMG signal ranges from 0.02 mV to 0.3 mV. In cases of ECG, EOG, and EMG, the amplitudes of the EP signals fall

around 0.4 mV, 0.1 mV and 20 μV respectively.

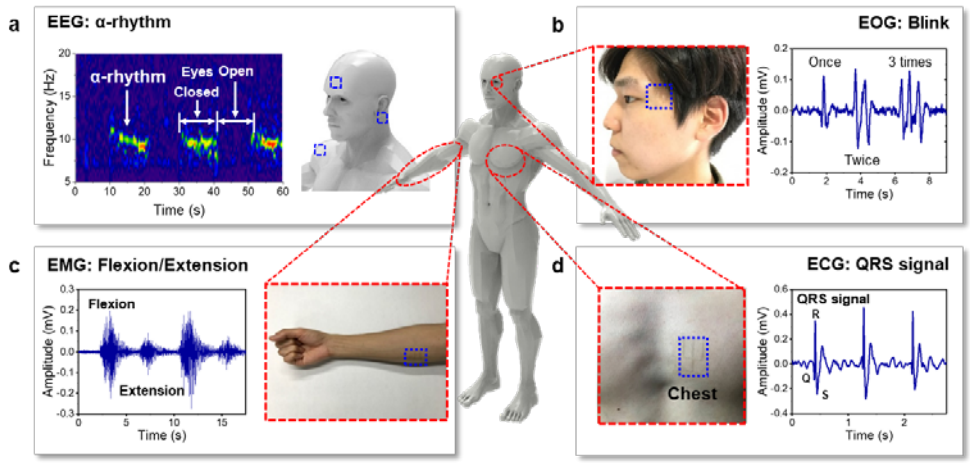

Figure 11. Various EP signal measurements using transparent kirigami EP sensor. Different EP signals from various locations for **a)** EEG, **b)** EOG, **c)** EMG, and **d)** ECG. Schematic illustration of measurement locations on graphical human model for monitoring EEG signal and EEG alpha-rhythms observed around 10 Hz in **a)**. Real images of measurement locations for other EP signals in **b-d)**.

3.4 Human-Machine Interface for Controlling a Quadrotor

Human-machine interface (HMI) demonstration using the TKE is crucial to exhibit because it refers that human body and computer/machine are closely linked by E-skin devices. **Figure 12** depicts human-machine interface for controlling a quadrotor drone (AR. Drone, Parrot SA, Paris) with using two sets of sEMG signals measured from specific gestures of both left/right forearms and wireless communication via Bluetooth and WiFi-network.

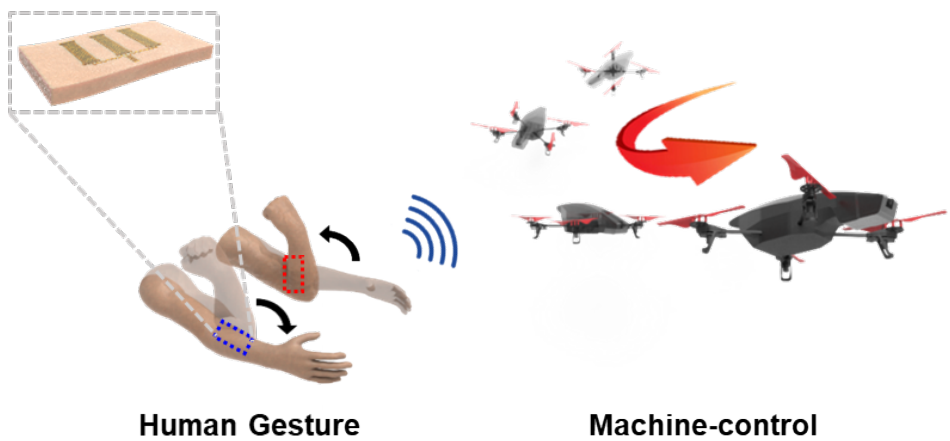

Figure 12. Human-machine interface using transparent kirigami electrodes. Schematic illustration of demonstrating HMI through TKEs by controlling a quadrotor with the gestures, which are signal-processed by Bluetooth and WiFi network.

Figure 13a shows the sets of sEMG signals measured from both forearms using the transparent kirigami EP sensors. Under the sEMG signals, roman numbers represent corresponding commands and quadrotor motions respect to command classification using sEMG signals for HMI are illustrated in **Figure 13b**. Generation of sEMG signals from flexor carpi in motions of flexion and extension is utilized to

control a quadrotor drone. Our bimanual gestures for commands include: (1) strong fists, (2) firm fists, (3) fists to the left, and (4) fists to the right. From the raw data produced by these motions, their root mean square (RMS) values are transferred using the equation (2), where n is the number of samples and x_k means the k^{th} sample.

$$RMS = \sqrt{\frac{1}{n}\sum_{k=1}^{n} {x_k}^2} \tag{2}$$

According to custom classification algorithm in MATLAB, the bimanual motions are paired with different five commands–Strong fists: “Take off and Land”, firm fists: “Fly forward”, fists to the left: “Turn left”, and fists to the right: “Turn right”. Before set to flight, we firstly analyze our sEMG signals on both channels of right and left forearms then establish discrete regions with boundary values for classifying commands with RMS values. The flight manipulation of a quadrotor is successfully demonstrated.

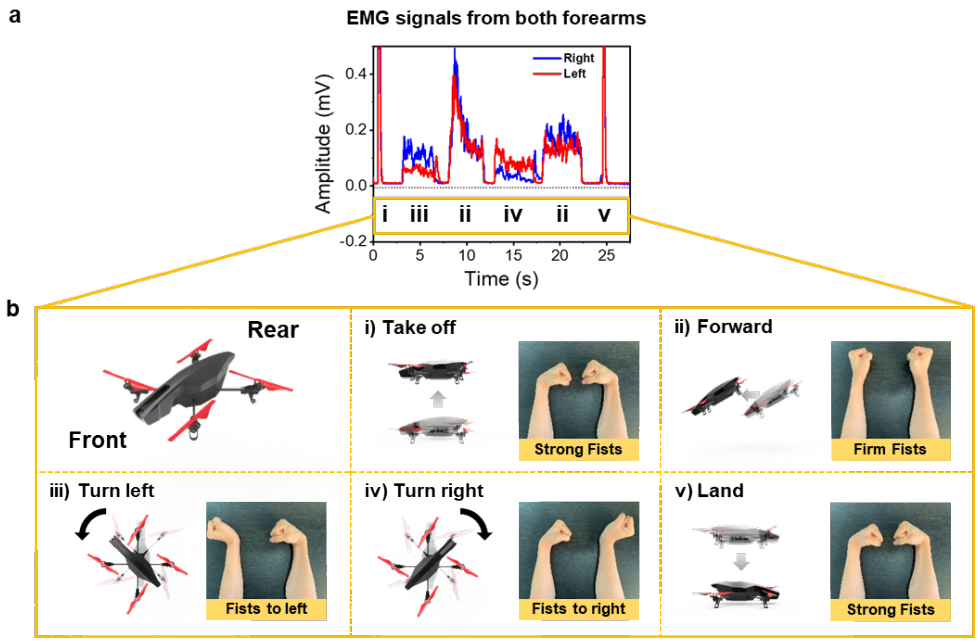

Figure 13. Demonstration of human-machine interface via transparent kirigami electrodes. a) Two measured EMG signals from both forearms using transparent kirigami EP sensors. Roman numbers enclosed in the orange box under the signals represent corresponding commands in **b)**. **b)** Description of control motions and corresponding gestures: i) Take off, ii) Fly forward, iii) Turn left, iv) Turn right, v) Land.

Chapter 4. Conclusion

In summary, we have reported a novel concept of transparent and stretchable kirigami electrodes consisting of ultra-thin and selectively Au-coated AgNWs/cPI nanocomposites with laser-patterned kirigami structure. The laser patterning technique provides digital and rapid process without requirement of patterning masks and fabrication steps in conventional photolithography process. By utilizing the laser patterning process, a configurable design of kirigami structures enable the transparent electrodes with tunable stretchability, which have strain limit from nearly zero strain to large strain over 400%. Biocompatibility and enhanced electrical stability against oxidation are attained by Au coating on the exposed surface of AgNWs, allowing stable electrothermal performance of the kirigami heater even at the elevated temperature of ~80 °C and long-term monitoring for various EP signals without skin irritations. Furthermore, owing to soft and ultra-thin but highly stretchable characteristic, our TKE conformally covers the curvilinear and irregular surfaces of human body, facilitating measurement of sEMG on both forearms with dynamic motions in real time for controlling a quadrotor in an advanced form for the demonstration of HMI. Based on these notable properties of TKE, these proposed concepts and approaches will open up various possibilities for accomplishing multi-functional transparent and wearable electronic skin applications with suitable geometries.

References

1 Yamada, T. *et al.* A stretchable carbon nanotube strain sensor for human-motion detection. *Nature nanotechnology* **6**, 296 (2011).

2 Jeong, J. W. *et al.* Materials and optimized designs for human-machine interfaces via epidermal electronics. *Advanced Materials* **25**, 6839-6846 (2013).

3 Yan, C. *et al.* Highly stretchable piezoresistive graphene–nanocellulose nanopaper for strain sensors. *Advanced materials* **26**, 2022-2027 (2014).

4 Miyamoto, A. *et al.* Inflammation-free, gas-permeable, lightweight, stretchable on-skin electronics with nanomeshes. *Nature nanotechnology* **12**, 907 (2017).

5 Gong, S. *et al.* A wearable and highly sensitive pressure sensor with ultrathin gold nanowires. *Nature communications* **5**, 3132 (2014).

6 Norton, J. J. *et al.* Soft, curved electrode systems capable of integration on the auricle as a persistent brain–computer interface. *Proceedings of the National Academy of Sciences*, 201424875 (2015).

7 Zhang, Y. *et al.* A mechanically driven form of Kirigami as a route to 3D mesostructures in micro/nanomembranes. *Proceedings of the National Academy of Sciences* **112**, 11757-11764 (2015).

8 Yeo, W. H. *et al.* Multifunctional epidermal electronics printed directly onto the skin. *Advanced Materials* **25**, 2773-2778 (2013).

9 Kim, D.-H. *et al.* Epidermal electronics. *science* **333**, 838-843 (2011).

10 Lee, C. H. *et al.* Soft core/shell packages for stretchable electronics. *Advanced Functional Materials* **25**, 3698-3704 (2015).

11 Kaltenbrunner, M. *et al.* An ultra-lightweight design for imperceptible plastic electronics. *Nature* **499**, 458 (2013).

12 Drack, M. *et al.* An imperceptible plastic electronic wrap. *Advanced Materials* **27**, 34-40 (2015).

13 Amjadi, M., Kyung, K. U., Park, I. & Sitti, M. Stretchable, skin-mountable, and wearable strain sensors and their potential applications: a review. *Advanced Functional Materials* **26**, 1678-1698 (2016).

14 Jang, K.-I. *et al.* Soft network composite materials with deterministic and bio-inspired designs. *Nature communications* **6**, 6566 (2015).

15 Someya, T., Bauer, S. & Kaltenbrunner, M. Imperceptible organic electronics. *MRS Bulletin* **42**, 124-130 (2017).

16 Hong, S. *et al.* Highly stretchable and transparent metal nanowire heater for wearable electronics applications. *Advanced materials* **27**, 4744-4751 (2015).

17 Fan, J. A. *et al.* Fractal design concepts for stretchable electronics. *Nature communications* **5**, 3266 (2014).

18 Kim, K. K. *et al.* Highly Sensitive and Stretchable Multidimensional Strain

Sensor with Prestrained Anisotropic Metal Nanowire Percolation Networks. *Nano Letters* **15**, 5240-5247, doi:10.1021/acs.nanolett.5b01505 (2015).

19 Someya, T. *et al.* Conformable, flexible, large-area networks of pressure and thermal sensors with organic transistor active matrixes. *Proceedings of the National Academy of Sciences* **102**, 12321-12325 (2005).

20 Someya, T. *et al.* A large-area, flexible pressure sensor matrix with organic field-effect transistors for artificial skin applications. *Proceedings of the National Academy of Sciences* **101**, 9966-9970 (2004).

21 Nawrocki, R. A., Matsuhisa, N., Yokota, T. & Someya, T. 300-nm Imperceptible, Ultraflexible, and Biocompatible e-Skin Fit with Tactile Sensors and Organic Transistors. *Advanced Electronic Materials* **2**, 1500452 (2016).

22 Brosteaux, D., Axisa, F., Gonzalez, M. & Vanfleteren, J. Design and fabrication of elastic interconnections for stretchable electronic circuits. *IEEE Electron Device Letters* **28**, 552-554 (2007).

23 Hsu, P.-C. *et al.* Personal thermal management by metallic nanowire-coated textile. *Nano letters* **15**, 365-371 (2014).

24 Choi, S. *et al.* Stretchable heater using ligand-exchanged silver nanowire nanocomposite for wearable articular thermotherapy. *ACS nano* **9**, 6626-6633 (2015).

25 Lee, H. B. *et al.* Mogul-Patterned Elastomeric Substrate for Stretchable Electronics. *Advanced Materials* **28**, 3069-3077 (2016).

26 Sekitani, T. *et al.* A rubberlike stretchable active matrix using elastic conductors. *Science* **321**, 1468-1472 (2008).

27 Zhang, Y. *et al.* Polymer-embedded carbon nanotube ribbons for stretchable conductors. *Advanced Materials* **22**, 3027-3031 (2010).

28 Kim, Y. *et al.* Stretchable nanoparticle conductors with self-organized conductive pathways. *Nature* **500**, 59 (2013).

29 Shyu, T. C. *et al.* A kirigami approach to engineering elasticity in nanocomposites through patterned defects. *Nature materials* **14**, 785 (2015).

30 Yang, S., Choi, I.-S. & Kamien, R. D. Design of super-conformable, foldable materials via fractal cuts and lattice kirigami. *MRS Bulletin* **41**, 130-138 (2016).

31 Blees, M. K. *et al.* Graphene kirigami. *Nature* **524**, 204 (2015).

32 Lamoureux, A., Lee, K., Shlian, M., Forrest, S. R. & Shtein, M. Dynamic kirigami structures for integrated solar tracking. *Nature communications* **6**, 8092 (2015).

33 Hong, S. *et al.* Selective laser direct patterning of silver nanowire percolation network transparent conductor for capacitive touch panel. *Journal of nanoscience and nanotechnology* **15**, 2317-2323 (2015).

34 Zhu, B. *et al.* Skin-inspired haptic memory arrays with an electrically reconfigurable architecture. *Advanced Materials* **28**, 1559-1566 (2016).

35 Jang, N.-S. *et al.* Simple Approach to High-Performance Stretchable Heaters

Based on Kirigami Patterning of Conductive Paper for Wearable Thermotherapy Applications. *ACS applied materials & interfaces* **9**, 19612-19621 (2017).

36 Jang, K.-I. *et al.* Rugged and breathable forms of stretchable electronics with adherent composite substrates for transcutaneous monitoring. *Nature communications* **5**, 4779 (2014).

37 Cheng, Y. *et al.* A Biomimetic Conductive Tendril for Ultrastretchable and Integratable Electronics, Muscles, and Sensors. *ACS nano* **12**, 3898-3907 (2018).

38 Wan, D., Xia, X., Wang, Y. & Xia, Y. Robust synthesis of gold cubic nanoframes through a combination of galvanic replacement, gold deposition, and silver dealloying. *Small* **9**, 3111-3117 (2013).

39 Liu, Q., Chen, J., Li, Y. & Shi, G. High-performance strain sensors with fish-scale-like graphene-sensing layers for full-range detection of human motions. *ACS nano* **10**, 7901-7906 (2016).

40 Lee, J. H., Lee, P., Lee, D., Lee, S. S. & Ko, S. H. Large-Scale Synthesis and Characterization of Very Long Silver Nanowires via Successive Multistep Growth. *Crystal Growth & Design* **12**, 5598-5605, doi:10.1021/cg301119d (2012).

41 Kim, H.-J., Sim, K., Thukral, A. & Yu, C. Rubbery electronics and sensors from intrinsically stretchable elastomeric composites of semiconductors and conductors. *Science advances* **3**, e1701114 (2017).

42 Lutey, A. H. An improved model for nanosecond pulsed laser ablation of metals. *Journal of Applied Physics* **114**, 083108 (2013).

43 Shyu, T. C. *et al.* A kirigami approach to engineering elasticity in nanocomposites through patterned defects. *Nat Mater* **14**, 785-789, doi:10.1038/nmat4327 (2015).

44 Xu, R. *et al.* Kirigami-inspired, highly stretchable micro-supercapacitor patches fabricated by laser conversion and cutting. *Microsystems & Nanoengineering* **4**, 36 (2018).

45 Lv, Z. *et al.* Editable supercapacitors with customizable stretchability based on mechanically strengthened ultralong MnO2 nanowire composite. *Advanced Materials* **30**, 1704531 (2018).

46 Hattori, Y. *et al.* Multifunctional skin-like electronics for quantitative, clinical monitoring of cutaneous wound healing. *Advanced healthcare materials* **3**, 1597-1607 (2014).

47 Samberg, M. E., Oldenburg, S. J. & Monteiro-Riviere, N. A. Evaluation of silver nanoparticle toxicity in skin in vivo and keratinocytes in vitro. *Environmental health perspectives* **118**, 407-413 (2009).

48 Mishra, S. *et al.* Soft, conformal bioelectronics for a wireless human-wheelchair interface. *Biosensors and Bioelectronics* **91**, 796-803 (2017).

49 Myers, A. C., Huang, H. & Zhu, Y. Wearable silver nanowire dry electrodes for electrophysiological sensing. *RSC Advances* **5**, 11627-11632 (2015).

국문 초록

Transparent Kirigami Electrodes for Electronic Skin Applications

박 정 재 (Jung Jae Park)
기계항공공학부 기계공학전공 (Mechanical Engineering)
Seoul National University

웨어러블 전자소자를 착용할 때 이질감을 최소화하기 위해 전자피부의 형태로서 사용되는 전극은 투명하여 눈에 잘 보이지 않아야 하고, 피부처럼 구부러지며 늘어날 수 있어야 한다. 하지만 전극의 재료와 구조적 측면에서 많은 연구가 진행되었음에도 여전히 투명하면서 늘어나는 전극을 구현하는 데 어려움이 많다. 본 논문에서는 이러한 어려움을 극복하기 위해 무색의 폴리이미드와 은 나노와이어를 기반으로 한 플렉서블 투명전극에 레이저 공정을 이용한 키리가미 패턴을 넣음으로써 스트레처블 투명전극을 구현하는 공정을 고안했다. 이를 바탕으로 본래 길이의 400% 까지 늘이는 반복인장시험을 10,000회 이상 진행한 후에도 저항변화가 거의 없는 투명전극을 제작했다. 또한 드러난 은 나노와이어의 표면에 선택적으로 금을 코팅함으로써 전극의 산화를 방지하고 생체에 부착 및 착용하기에 적합할 수 있도록 했다. 본 연구에서는 이를 이용해 용도에 맞게 디자인된 키리가미 패턴을 가진 투명전극을 적용한 웨어러블 히터와 생체신호 측정센서를 제작했다. 더 나아가 근전도 센서를 양팔에 부착한 후 역동적인 움직임에 대응되는 근전도 신호를 읽어 쿼드로터를 조종하는 시스템을 구축함으로써 진보된 인간-기계 인터페이스를 구현했다.

Keyword : 투명, 컨포멀, 스트레처블 전자소자, 은 나노와이어, 전자피부

Student Number : 2017-20632